

THE RESPONSE OF THE HUMAN VISUAL SYSTEM TO MOVING SPATIALLY-PERIODIC PATTERNS: FURTHER ANALYSIS

DAVID H. FOSTER

Applied Optics Group, Physics Department, Imperial College, London, S.W.7

(Received 8 May 1970)

INTRODUCTION

THE PRINCIPAL characteristics of a visual motion response associated with certain classes of moving stimuli, and the elements of a mathematical model describing the system in that response have been given in an earlier report (FOSTER, 1969). It is the purpose of the present investigation to extend this study, both experimentally and theoretically.

First, the main findings of the earlier work are reviewed.

It has been demonstrated (FOSTER, 1968) that in the perception of moving, spatially-periodic patterns, there exist transitions in sensation associated with certain critical values of the temporal frequency, f , the angular area, θ , and the spatial period, λ , of the stimulus. Thus, if the temporal frequency of the stimulus is the controlled variable, we have the following:

- (i) For $f \leq f_l$ (the lower critical frequency)—a sensation of well defined, directed motion,
- (ii) for $f_l < f \leq f_u$ (the upper critical frequency)—a sensation of non-directed motion, or flicker,
- (iii) for $f > f_u$ —fusion.

At certain values of the input parameters, a stationary stroboscopic effect is also observed.

Using a rotating radial grating as the primary stimulus, and restricting the field of view to a foveal annulus, the interrelationships of the variables, f_u , f_l , θ , and λ , were investigated (FOSTER, 1969). Square waveform gratings, only, were employed.

A typical set of curves, obtained for the author, is shown in Fig. 1.

The most significant results of this investigation are summarized below:

- (i) The variation of the upper critical frequency, f_u , with angular area, θ , is independent of the spatial period, λ , including the limiting case, $\lambda = \infty$. (The latter is equivalent to a spatially uniform flashing source.)
- (ii) The variation of the lower critical frequency, f_l with angular area, θ , is not independent of λ , and at fixed θ , f_l decreases with increasing λ (q.v. Fig. 1).
- (iii) The stationary stroboscopic effect (marked "s" in Fig. 1) occurs when $\theta > \lambda/2$, for all $\lambda < 180^\circ$.
- (iv) The visual response at motion threshold is insensitive to the phase structure of the stimulus pattern (at $\theta = 360^\circ$).

On the basis of these observations, the following conclusions were drawn, concerning the nature and organization of the information processing elements present in the human visual system.

(i) There exist two types of information processing unit: a vertical (V) unit, which deals with local temporal fluctuations of the stimulus, and a horizontal (H) unit, which deals with the spatial ordering of these local temporal fluctuations. These units are replicated across the visual field as shown in Fig. 2.

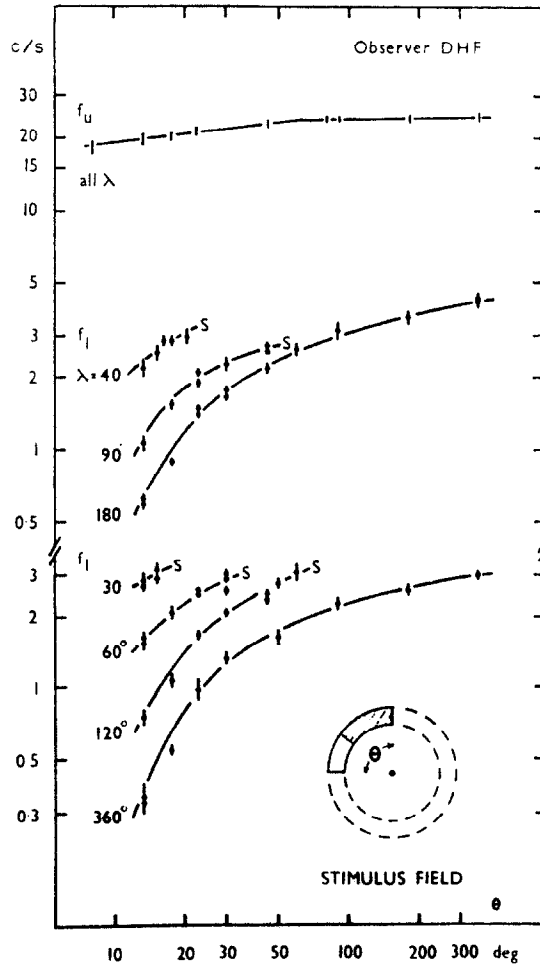


FIG. 1. Curves showing the variation of the upper critical frequency, f_u , and lower critical frequency, f_l , with angular area, θ , and spatial period, λ . The onset of the stationary stroboscopic effect is indicated at the points marked "s". The root mean square deviation associated with each reading is shown by the vertical bars.

(ii) The V -unit was identified with the de Lange filter (DE LANGE, 1954). This describes the frequency response of the human visual system at flicker-fusion threshold.

(iii) The H -unit was identified with some form of Reichardt multiplier (REICHARDT and VARJU, 1959, see Fig. 3a). This was originally developed in order to describe the optomotor

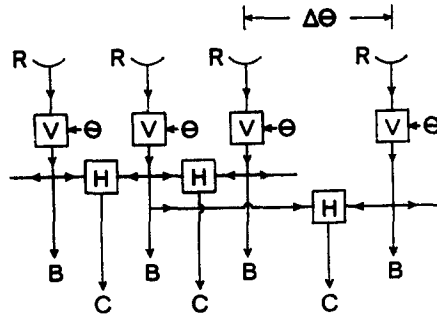
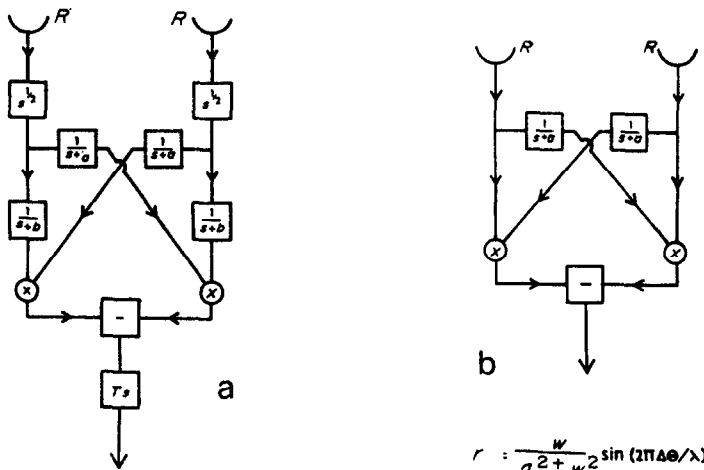


FIG. 2. The organization of the information processing elements: *R* are receptor (or groups of receptors), *V* are de Lange low pass filters, and *H* are Reichardt multipliers (see text). The channels marked *B* carry information about local temporal fluctuations of the stimulus, and those marked *C* carry information about the spatial ordering of these local temporal fluctuations. The angular area, θ , is included as a parameter in the *V*-unit description.

response of the beetle *Chlorophanus*. The response of the multiplier to sinewave inputs is given below:

$$r = \frac{kw^2}{(a^2 + w^2)(b^2 + w^2)} \cdot \sin(2\pi \cdot \Delta \theta / \lambda) \quad (1)$$

where $w = 2\pi f$,
 a, b and k are real positive constants,
 $\Delta \theta$ is the input (receptor) pair separation,
 and λ is the spatial period of the stimulus.



$$r = \frac{kw^2}{(a^2 + w^2)(b^2 + w^2)} \sin(2\pi \Delta \theta / \lambda)$$

FIG. 3. Complex frequency (*s*) domain representation of two-element movement detectors. In (a) is shown the Reichardt multiplicative interaction scheme (T_s is a time averaging element). In (b), is shown Thorson's simplification of the Reichardt scheme. The sinewave response of each system is indicated.

[It may be seen that for $\Delta\theta > \lambda/2$ (and $\Delta\theta < 2$) the motion response r is negative. It may also be shown (REICHARDT and VARJU, 1959) that the response is insensitive to the phase structure of the stimulus pattern.]

(iv) Summation/threshold mechanisms associated with the V -unit output channels were shown to spatially phase insensitive in their action. In the case of the H -unit system, it was concluded that positive and negative outputs from different units do not undergo "arithmetic" summation. Since negative outputs only arise when $\Delta\theta > \lambda/2$ (see above), this was shown to provide an explanation of the stationary stroboscopic effect.

(v) The maximum input (receptor) pair separation, measured angularly around the annular field, was deduced to be between 60° and 90° .

Using the system outlined above, it was shown possible to describe, in a qualitative fashion, the observed characteristics of the visual response to certain moving, spatially-periodic stimuli.

In order to provide a quantitative description of the observed motion response data, the construction of the functional units making up the system model must be specified in greater detail. Thus, it is necessary to determine the modification of the Reichardt multiplier most appropriate in the H -unit description, the frequency response characteristics of the V -units, and the dependence of the response upon the number of units operating (a function of θ).

In contrast to the earlier investigation (FOSTER, 1969), both sine and square wave stimuli are used in the present study, and experimental observations are extended to four subjects (including the author). The general experimental approach is the same, however, and "small-signal" stimuli are employed to prescribe system linearity (q.v. THORSON, 1966).

APPARATUS AND METHODS

Referring to Fig. 4, the primary stimulus consisted of a rotating radial grating, RG , transilluminated by the incandescent lamp, L_1 , via the liquid filter, F , and flashed opal diffusing screen, D_1 . The view of the grating was restricted, with the mask, M_1 , to an annulus of 1.5° total mean angular subtense, and angular width, 0.21° . Portions of the annulus could be sectioned off; the remaining sector was specified by the angular coordinate, θ (see inset of Fig. 4).

A rectangular background field, uniform to within 5 per cent and of total angular subtense, 4.7° , was provided by the light box, L_2 , and diffusing screen, D_2 . In front of D_2 was placed the mask, M_2 , the complement of M_1 .

The primary stimulus field and background field were combined with the beam splitter, P , and the demagnified whole viewed via a 2 mm artificial pupil, AP . Retinal illumination was approximately 390 trolands, and the colour temperature of the background field, approximately 2500°K.

The radial grating was driven by an electric motor via a system of gears; grating speeds of from 0.1 rev/sec to 40 rev/sec could thus be obtained. Angular velocities were monitored continuously using an electronic tachometer.

Both square and sinewave radial gratings were employed. The square wave gratings consisted simply of sectorised discs, with spatial periods ranging from 40° to 360° . The sinewave gratings were approximated by discs consisting of constant thickness radii, the angular separation of which was proportional to the mean angular coordinate (see Fig. 4). The high frequency content of these sine-approximated gratings was reduced, *in situ*, by placing a second diffusing surface between the grating and the prism. Using this method, nominal sine gratings with spatial periods of 180° and 360° , were prepared. [The harmonic contents of both square and sinewave gratings were checked, and deviations from the ideal waveforms shown to be within experimental tolerances (FOSTER, 1970).]

To provide the required small-signal operating conditions, a 10 per cent neutral density filter was inserted between the grating and the prism.

General experimental procedure

A dental bite was used to locate the head of the subject, who fixated, monocularly, the centre of the annular stimulus. The speed of rotation of the grating could be controlled by the observer.

In order to define a fixed-coordinate, input (receptor) array, it was necessary to ensure good fixation. Two criteria were used to judge when such fixation ceased:

- (i) The disturbance of the gradual trend of the stimulus sensation to that of steady state.
- (ii) The interruption of the gradual "washing-out" of the surround field (see RIGGS, RATLIFF, CORNSWEET and CORNSWEET, 1953).

Sharp eye movements, or flicks (q.v. DITCHBURN and GINSBORG, 1953), could also be identified by the sudden brightening of some dark contours which formed part of the fixation spot (q.v. LORD and WRIGHT, 1950). [Residual eye tremor (see DITCHBURN and GINSBORG, 1953) was not thought to be significant, in view of the findings of WEST (1968) and GILBERT and FENDER (1969). West showed that the temporal frequency response, at fusion threshold, remains of the same form both in stabilized and non-stabilized vision. Gilbert and Fender demonstrated a similar result for the spatial frequency response characteristics.]

Before commencing observations, the stimulus intensity was standardized against the background field intensity. The stimulus pattern (fused by the observer) was superimposed on the negative mask, M_2 , (q.v. Fig. 4) and the two fields matched for colour and brightness with the liquid filter, F . M_2 was then

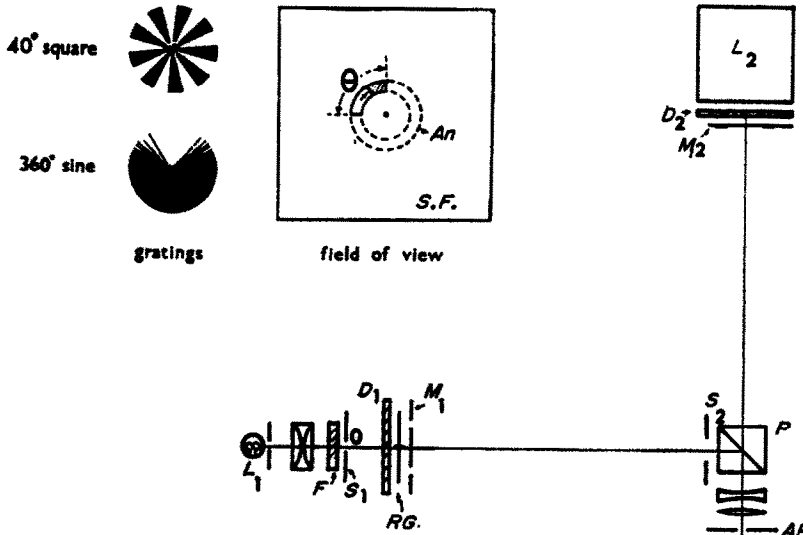


FIG. 4. The experimental apparatus: L_1 and L_2 are incandescent light sources; F , a liquid filter for colour correction; S_1 and S_2 , stops; D_1 and D_2 , diffusing screens; RG , radial grating, M_1 and M_2 , positive and negative masks; P , split prism; AP artificial pupil. In the inset: sine and square wave radial gratings, and the field of view. An is the annular aperture, and SF , the surround field.

removed, leaving a uniform background field, and the 10 per cent neutral density filter reintroduced between grating and beam splitter. Thus, the stimulus intensity variation was within 10 per cent of the background (mean) intensity, and superimposed upon it.

Observers employed were the author (DHF) who wore correcting contact lenses and was aged 24 years, GF who was 20 years old and was slightly myopic (a correcting lens was introduced), RAE who was emmetropic and 22 years old, and WHK who was also emmetropic and 42 years old.

EXPERIMENTS AND RESULTS

As in the previous investigation (FOSTER, 1969), the general characteristics of the system were first examined. Thus, the uniformity in the motion response around the annular field, and the symmetry of the motion response with respect to reversal of stimulus direction were established for each of the observers.

The dependence of the lower critical frequency on angular area, spatial period and waveform

The lower critical frequency, f_1 , was determined as a function of the angular area, θ , with grating periods, λ , ranging from 40° to 360° for the square wave stimulus, and 180° and 360° for the sine wave stimulus.

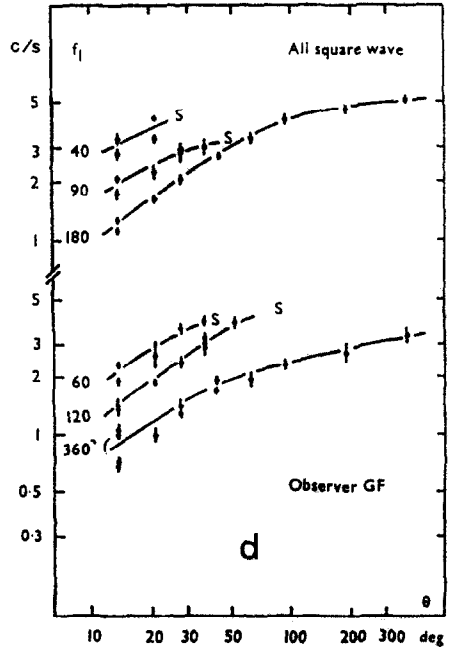
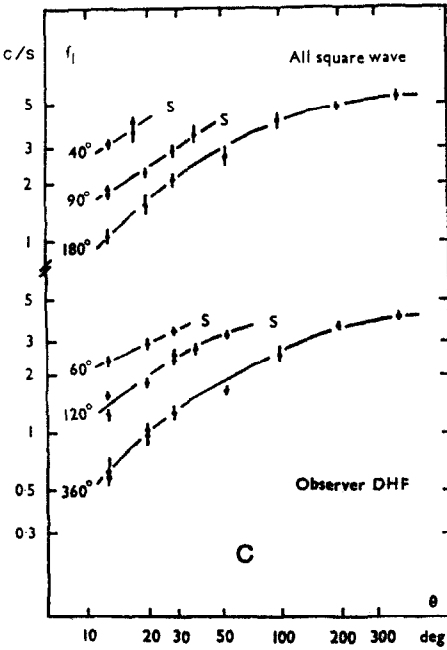
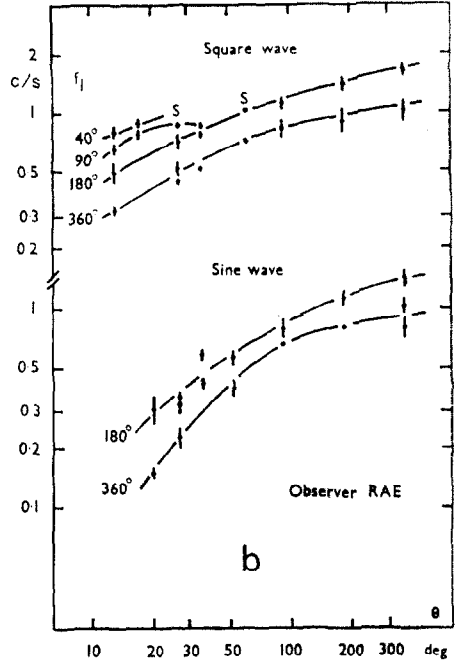
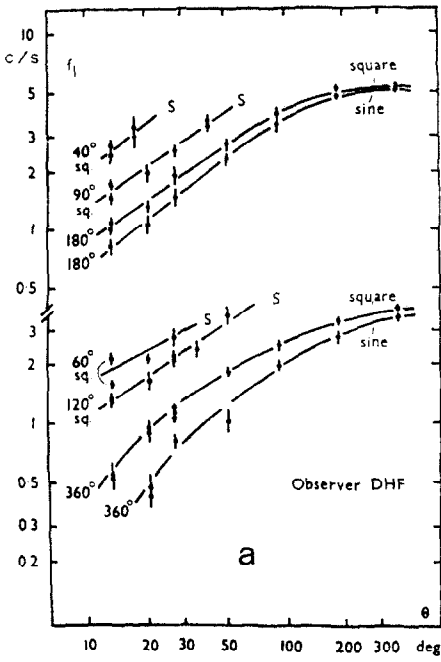


FIG. 5.

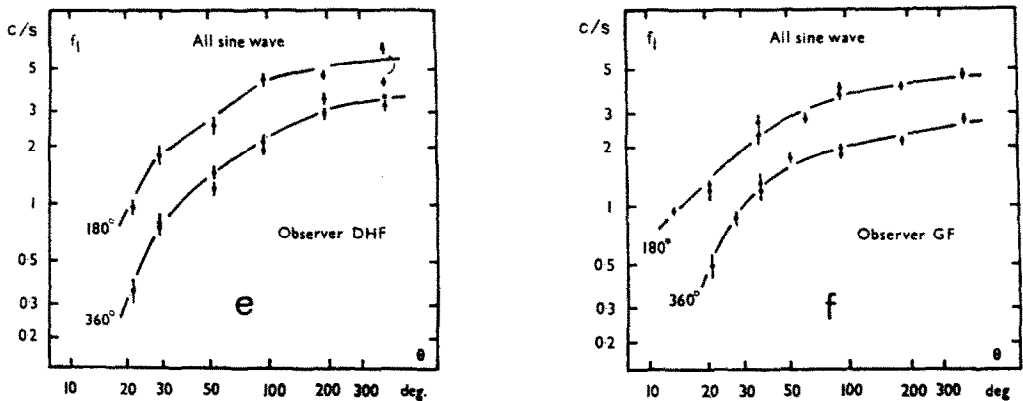


FIG. 5. The variation of the lower critical frequency, f_l , with angular area, θ , and spatial period, λ . Both sine and square wave responses are displayed, with the onset of the stationary stroboscopic effect indicated at the points marked "s". The root mean square deviation associated with each point is also shown.

The recorded data of Figs. 5a–5f show the general upward trend of f_l with both increasing θ and decreasing λ (q.v. Fig. 1). The sine response curves are depressed with respect to those for square wave stimuli, the difference being most marked at low f_l values. The onset of the stationary stroboscopic effect is indicated at points marked "s" and is seen to occur for all λ values tested, except for $\lambda = 180^\circ$ and $\lambda = 360^\circ$. It is also noted that at the onset of the stationary stroboscopic effect, the angular area, θ , is approximately equal to half the spatial period, $\lambda/2$.

The dependence of the upper critical frequency on angular area, and spatial period

The upper critical frequency, f_u , was also determined as a function of the angular area of the stimulus, θ , for a range of grating periods, λ . Square waveform gratings were used only.

The results obtained are displayed in Fig. 6. For each λ value, the corresponding curve has been displaced for ease of examination. Included as a limiting case (in Fig. 6a) is that of f_u vs. θ for infinite spatial period. It is noted that the f_u vs. θ response is independent (within experimental error) of the spatial period.

The de Lange low frequency attenuation characteristics

To determine the modulation transfer function of the V-units, i.e. the de Lange flicker-fusion attenuation characteristics, the following procedure was adopted.

The 360° sine wave grating was arranged to interrupt the primary stimulus at the inter-mediated focus, O , of the source, L_1 (Fig. 4). (This produced a spatially uniform field, with temporal modulation only.) A neutral, variable density wedge was placed in front of the stop S_2 , and the fixed 10 per cent neutral density filter removed. With the temporal frequency of the stimulus fixed by the experimenter the transmission of the wedge was adjusted by the subject so that flicker could just be discerned.

Note. The primary stimulus was superimposed on the background field, and therefore changes in stimulus modulation depth result in changes in the total mean intensity level. These departures from fixed level working conditions were restricted to 10 per cent of the background level by limiting the range of modulation depths available. Only low frequency response characteristics could therefore be determined (see DE LANGE, 1954).

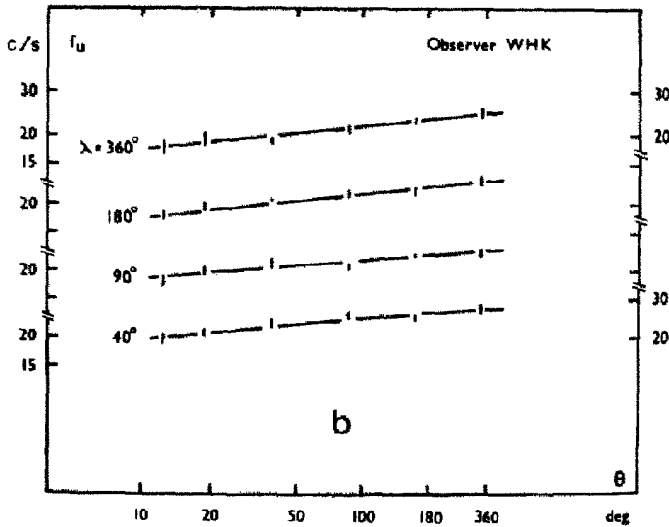
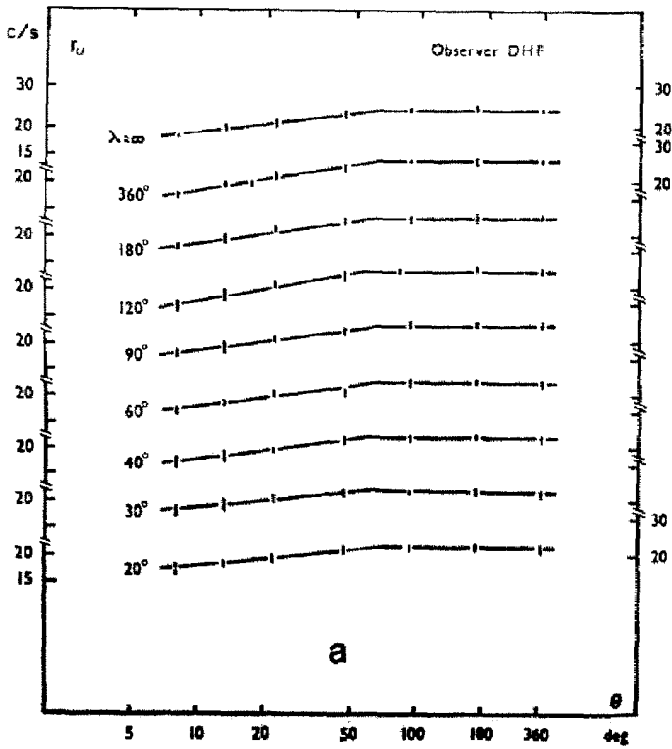


FIG. 6. The variation of the upper critical frequency, f_u , with angular area, θ , and spatial period, λ . All waveforms are square, and the rms deviation associated with each point is indicated.

Using the above method, low frequency attenuation characteristics were obtained for angular areas, θ , ranging from 13° to 360° . In Fig. 7, results for three observers are shown. Each curve has been displaced vertically for ease of examination.

It will be seen that there is no well-defined change in shape of the characteristics with variation in area, apart from a bodily downward shift with decreasing θ . Significant attenuation does not commence until the temporal frequency exceeds 9 c/s.

ANALYSIS

Some general comments are first made concerning the validity of the conclusions reached in the earlier study on the visual motion response (FOSTER, 1969).

(i) The initial analysis of the response of the visual system to moving, spatially-periodic stimuli was based primarily on the results of one subject (DHF). From Figs. 5 and 6 it may be seen that the general characteristics of the f_i vs. θ , λ and the f_u vs. θ , λ responses are indeed common to all subjects tested.

(ii) It was argued that the higher harmonics of the square wave stimulus are not significant (to a first approximation) in determining the form of the motion response. This conclusion is supported by the results of Fig. 5, in which it is seen that the sine wave motion response only differs markedly from the square wave motion response at very low f_i values.

Thus, the initial experimental evidence for the form of the visual motion response, and the deductions based upon this evidence, are given further weight; the conclusions outlined in the Introduction, concerning the make-up of the system model, are therefore taken as the starting point for the following analysis.

The intention is to give a detailed mathematical structure to the model. Specifically, we obtain a simplified description of the V -unit, and deduce the form of the areal dependence of the V -unit summation/threshold system. The nature of the H -unit output interaction is examined further, and an expression is derived for the general response of the model at motion threshold. The sinewave motion response data is then fitted.

It is shown necessary to modify the basic Reichardt scheme in order to reconcile the theoretical square wave motion response of the model with the observed data. The resulting expression for the square wave motion response is then used to arrive at a value for the minimum input (receptor) pair separation, $\Delta\theta_{\min}$.

Some predictions of the model are also briefly discussed.

The V -units

It has been shown (FOSTER, 1969) that the V -units may be identified with de Lange filters. Since the de Lange attenuation characteristics of Fig. 7 are area dependent, the angular area, θ , must be included as a parameter in the V -unit specification (see Fig. 2).

We now show that this description may be simplified.

Referring to Fig. 7, we see that the de Lange characteristics do not exhibit a well-defined change in shape with area, θ , although there is a downward shift of the curves with reduction in θ . Thus, to a first approximation, the shape of the characteristics (attenuation vs. frequency) may be considered to be independent of θ . If the sensitivity of the system to variations in θ is then attributed solely to threshold variations, which simply shift the fundamental frequency response along the attenuation axis, θ may be eliminated from the V -unit description.

Let $W(w)$ ($w = 2\pi f$) represent the θ -independent frequency response characteristics of the V -unit. To determine $W(w)$, the following was carried out.

Each of the de Lange attenuation characteristics, determined for a particular θ value, is

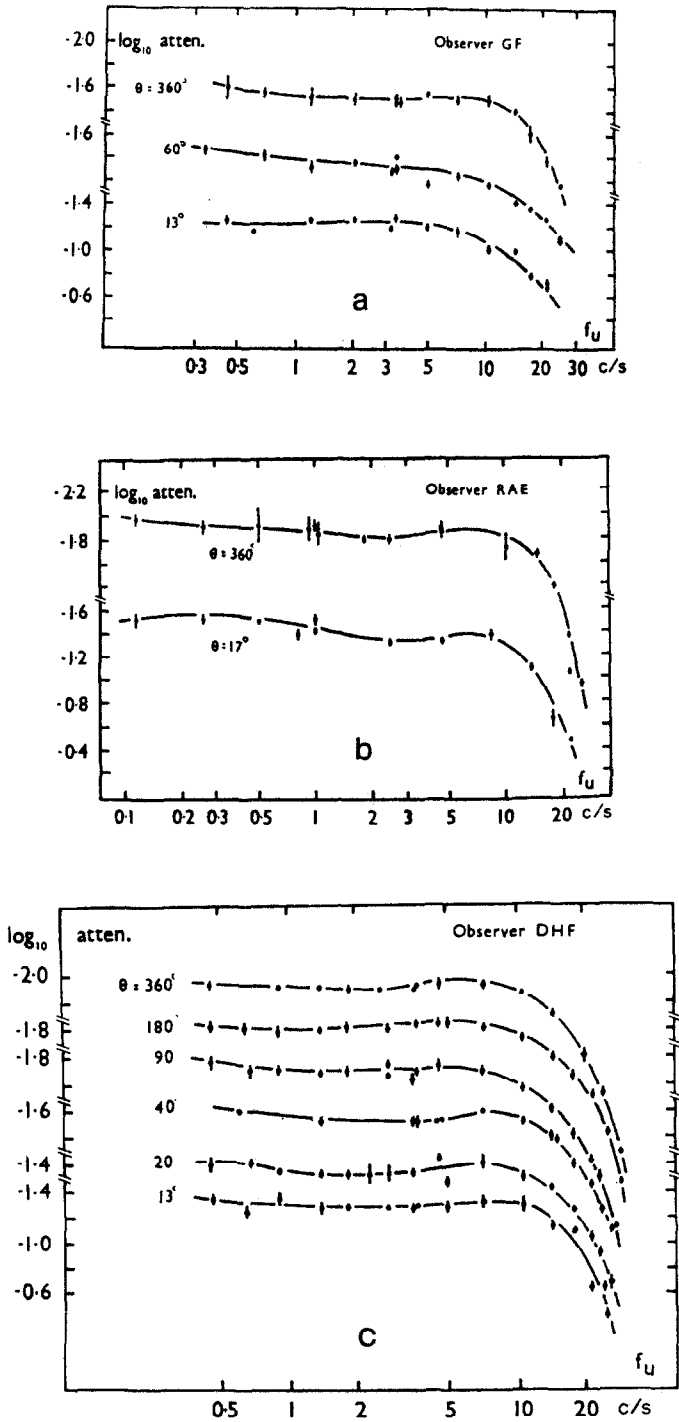


FIG. 7. The de Lange low frequency attenuation characteristics at various values of the angular area, θ , (see text). The rms deviation associated with each point is indicated.

shifted vertically to set the attenuation equal to zero at low frequencies, and the curves then superimposed. The averaged response function, thus obtained, is shown in Fig. 8. These curves define the V -unit attenuation characteristics $W(w)$ for the present experimental configuration.

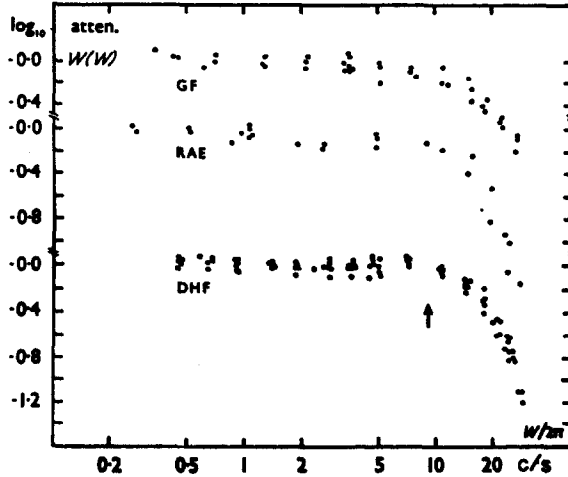


FIG. 8. The θ -independent frequency response characteristics of the V -units (see text). w is the temporal angular frequency.

The summation/threshold units associated with the V-units

Two possible types of summation/threshold arrangement, associated with the V -units, have been defined (FOSTER, 1969); viz:

Scheme (a) in which the V -unit outputs retain their separateness, and feed directly into individual threshold units.

Scheme (b) in which the V -unit outputs first feed into a phase-independent summation unit. The output of this unit then feeds into a single threshold unit.

The areal (θ) dependence of the system, in case (a), is located at each threshold unit, and in case (b), is located at the summation unit. With the data available, it is not possible to distinguish between the two systems, (a) and (b).

The specific areal (θ) sensitivity of the system ($P_V(\theta)$, say) is obtained from the experimental data of Fig. 7, by plotting the attenuation at the lowest temporal frequency ($f_n = 0.45$ c/s) as a function of the angular area, θ . For DHF only six θ values are available (Fig.

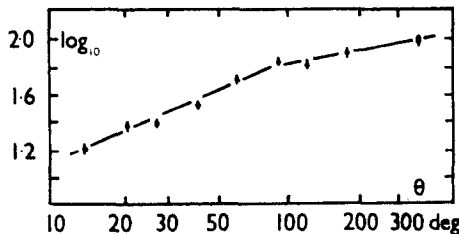


FIG 9. The areal sensitivity, $P_V(\theta)$, of the V -unit summation/threshold system (see text). (rms Deviation associated with each point is indicated.)

7), and therefore to determine a more precise value of the areal weighting factor, $P_V(\theta)$, direct measurement of the flicker threshold as a function of θ , at $f_u = 0.45$ c/s, was carried out. The same methods were used as in the determination of the de Lange characteristics, described earlier.

The results of these measurements are shown in Fig. 9 (for one subject). This curve defines for the present experimental configuration the areal sensitivity, $P_V(\theta)$, of the V -unit summation/threshold mechanisms.

The H -units and associated summation/threshold units

In this section, we distinguish two possible types of summation/threshold mechanism associated with the H -units, and obtain a general statement describing the response of the model at motion threshold. The significance of the angular area, θ , and input (receptor) pair separation, $\Delta\theta$, in weighting the H -unit outputs is evaluated, and a theoretical expression for the sinewave f_i vs. θ response is derived.

First, two possible summation/threshold mechanisms are examined.

In proposing the origin of the stationary stroboscopic effect (FOSTER, 1969), it was necessary to postulate that the outputs of the H -units do not undergo "arithmetic" summation, in order that positive and negative motion response contributions remain distinct. However, the sign of the H -unit response only depends upon the input pair separation, $\Delta\theta$, (see equation 1), and therefore the above restriction only applies to H -units with different $\Delta\theta$. For H -units with identical $\Delta\theta$, there is no such restriction, and the same two possibilities exist for output interaction as for the V -units.

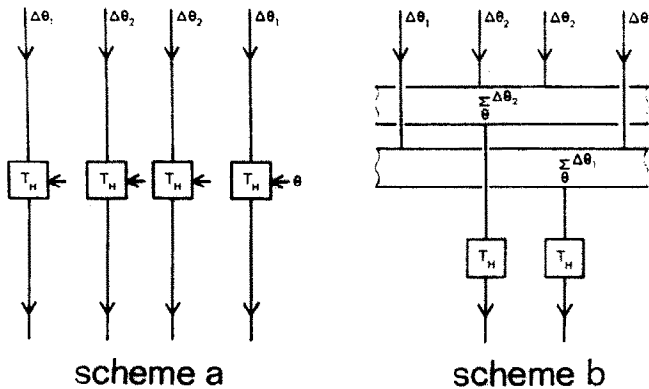


FIG. 10. Two possible H -unit summation/threshold systems. In (a), every channel, independent of $\Delta\theta$ origin, has an associated threshold unit, T_H , which is modified in behaviour by θ . In (b) outputs from H -units with identical $\Delta\theta$ first undergo phase independent summation, before passing into θ -independent threshold units (see text).

Thus, referring to Fig. 10a, the H -unit outputs retain their separateness, even within a group of identical H -unit $\Delta\theta$. Each channel, independent of $\Delta\theta$ origin, has an associated threshold unit, T_H , which is modified in behaviour by the angular area, θ . Alternatively, in Fig. 10b, those H -unit outputs with identical $\Delta\theta$ first feed (via some areal weighting factor) into the phase-independent summation unit, $\frac{\sum \Delta\theta}{\theta}$. In turn, the single outputs from each of the summation units, associated with a particular $\Delta\theta$, feed into a single associated threshold unit, T_H .

As with the V -unit summation/threshold schemes, the areal (θ) dependence of the H -unit summation/threshold system is located, in case (a), at each threshold unit, and in case (b), at the summation unit.

Let this areal sensitivity of the system be represented by the function $P_H(\theta)$; i.e. $P_H(\theta)$ describes the sensitivity of the response to variations in the total number of H -units operating. Suppose there also exists a relative weighting of the H -unit output, with input (receptor) pair separation, $\Delta\theta$, and that this is described by the function, $p_H(\Delta\theta)$; i.e. $p_H(\Delta\theta)$ describes the sensitivity of the response to variations in the H -unit population with input separation, $\Delta\theta$. Then at some θ , w , λ , ($w = 2\pi f$), the final weighted output, $r'_{\theta w \lambda}(\Delta\theta)$ say, of a *single* H -unit by scheme (a), or of a group of H -units by scheme (b), is defined by the following expression:

$$r'_{\theta w \lambda}(\Delta\theta) = P_H(\theta) \cdot p_H(\Delta\theta) \cdot r_{w \lambda}(\Delta\theta) \quad (2)$$

where $r_{w \lambda}(\Delta\theta)$ is the response of a single H -unit.

The final output, describing the total motion response, consists of all those weighted outputs, $r'_{\theta w \lambda}(\Delta\theta)$, which are each large enough to surmount the associated motion threshold, T_H . For a sensation of *directed* motion to be elicited, it is also required that all $r'_{\theta w \lambda}(\Delta\theta)$ have the same sign (q.v. FOSTER, 1969).

Now as the temporal frequency is increased, $r_{w \lambda}(\Delta\theta)$, and therefore $r'_{\theta w \lambda}(\Delta\theta)$, decrease in magnitude (q.v. equation 1). It therefore follows that, providing all $r'_{\theta w \lambda}(\Delta\theta)$ have the same sign, the greatest frequency at which there exists at least one $r'_{\theta w \lambda}(\Delta\theta) > T_H$, is the lower critical frequency, f_i ($f_i = w/2\pi$).

Thus, in order for a well-defined directed sensation of motion to be just perceived, we require that all $r'_{\theta w \lambda}(\Delta\theta)$ have the same sign, and that

$$r'_{\theta w \lambda}(\Delta\theta)_{\max} = T_H \quad (3)$$

where the maximum value, referred to above, is with respect to the $\Delta\theta$ values available, viz. $\Delta\theta_{\min}$ to $\Delta\theta_{\max}$.

In order to determine the relationship between θ , w , and λ such the above threshold condition is satisfied, equation 2, describing the weighted H -unit output, must first be expanded. That is, the following factors must be obtained in more explicit form.

(i) $r_{w \lambda}(\Delta\theta)$, i.e. the output, at some w , λ of an H -unit with input (receptor) pair separation, $\Delta\theta$.

(ii) $P_H(\theta)$, i.e. the areal weighting factor associated with the H -unit outputs.

(iii) $p_H(\Delta\theta)$, i.e. the relative weighting factor associated with the H -unit outputs.

The above factors are now evaluated.

(i) It may be shown (FOSTER, 1970) that of the various modifications of the basic Reichardt scheme available, the most appropriate version in the present analysis is that due to THORSON (1966), Fig. 3b. (It has also been previously demonstrated [FOSTER, 1969] that this version provides an adequate description of the f_i vs. θ response at $\theta = 13^\circ$.) Therefore, the response of the H -unit, $r_{w \lambda}(\Delta\theta)$, may be determined for any input waveform. (The sinewave response is given in Fig. 3b.)

(ii) It has also been shown (FOSTER, 1969) that there exists a maximum value to the H -unit input pair separation, viz. $\Delta\theta_{\max}$. It therefore follows that for $\Delta\theta > \Delta\theta_{\max}$, the relative weighting factor, $p_H(\Delta\theta)$, must be zero. Furthermore, since the f_i vs. θ curves for $\lambda = 180^\circ$ and $\lambda = 360^\circ$ are monotonic (q.v. Figs. 5a-f), $p_H(\Delta\theta)$ must also be monotonic. There-

fore from the above $p_H(\Delta\theta)$ must fall off smoothly to zero. In practice we might choose something of the form:

$$p_H(\Delta\theta) = \frac{1}{\Delta\theta^m} \quad m \gtrsim 1, \quad \text{for } \Delta\theta \leq \Delta\theta_{\max}. \quad (4)$$

$$= 0, \quad \text{for } \Delta\theta > \Delta\theta_{\max}.$$

(iii) We now determine the form of the areal weighting factor, $P_H(\theta)$, and at the same time, obtain an explicit expression for the sinewave response of the system at motion threshold.

Since Thorson's modification (Fig. 3b) of the Reichardt scheme has been chosen to represent the H -unit function, we have for sinewave inputs:

$$r_{w\lambda}(\Delta\theta) = \frac{w}{a^2 + w^2} \cdot \sin(2\pi \cdot \Delta\theta/\lambda). \quad (5)$$

Note. The attenuation due to the V -units may be omitted. This is possible since we are dealing with sinewave stimuli, for which $f_i < 9.0$ c/s (see Fig. 5); significant attenuation by the V -units does not commence until $f_i > 9.0$ c/s (see Fig. 8).

Substituting $r_{w\lambda}(\Delta\theta)$, defined by equation 5, and $p_H(\Delta\theta)$, defined by equation 4, into equation 2, giving the weighted H -unit output, we obtain the following:

$$r'_{\theta w\lambda}(\Delta\theta) = P_H(\theta) \cdot \Delta\theta^{-m} \cdot \frac{w^2}{a^2 + w^2} \cdot \sin(2\pi \cdot \Delta\theta/\lambda). \quad (6)$$

In order to reduce the above expression for the H -unit sinewave response to a threshold statement of the form of equation 3, it is first necessary to show that all H -unit outputs have the same sign; we may then determine the maximum value of $r'_{\theta w\lambda}(\Delta\theta)$, defined by equation 6, with respect to $\Delta\theta$.

Now, $\Delta\theta_{\max} < 90^\circ$ (see Introduction), and therefore for $\lambda = 180^\circ$ and 360° , $\sin(2\pi \cdot \Delta\theta/\lambda)$ is positive for all values of $\Delta\theta$. Thus, the condition that all H -unit outputs have the same sign is satisfied for the range of sine gratings employed.

Secondly, referring to equation 6, it may be seen that the maximum value of $[\Delta\theta^{-m} \cdot \sin(2\pi \cdot \Delta\theta/\lambda)]$ occurs at $\Delta\theta = \Delta\theta_{\min}$, providing $m \geq 1$ (the actual value of $\Delta\theta_{\min}$ has yet to be determined).

Thus, from the above, equation 6 gives rise to the following threshold statement:

$$P_H(\theta) \cdot \Delta\theta_{\min}^{-m} \cdot \frac{w^2}{a^2 + w^2} \cdot \sin(2\pi \cdot \Delta\theta_{\min}/\lambda) = T_H \quad (7)$$

and since $\Delta\theta_{\min}^{-m}$ is constant, it may be incorporated into the constant, T_H , giving:

$$P_H(\theta) \cdot \frac{w^2}{a^2 + w^2} \cdot \sin(2\pi \cdot \Delta\theta_{\min}/\lambda) = T_H. \quad (8)$$

The above expression defines the relationship between the temporal frequency, f_i ($f_i = 2\pi w$), the angular area, θ , and the spatial period, λ of the sinewave stimulus at motion threshold.

We now obtain the form of the areal weighting factor, $P_H(\theta)$.

It can be shown (FOSTER, 1970) that the rate constant, a , is only significant at low values of w , and for the sinewave response at $\lambda = 180^\circ$, may be ignored. If the $\lambda = 180^\circ$ response, only, is considered, $\sin(2\pi \cdot \Delta\theta_{\min}/\lambda)$ is then constant.

Therefore, for the $\lambda = 180^\circ$ sinewave response, equation 8 simplifies to the approximation below:

$$P_H(\theta) \simeq \text{constant} \cdot f_i(\theta) \quad (9)$$

where w has been replaced by f_i .

Thus, the $\lambda = 180^\circ$, f_i vs. θ sine response curve gives a direct measure of the areal weighting factor, $P_H(\theta)$.

It will be demonstrated later that $P_H(\theta)$ may be approximated by the power function:

$$\begin{aligned} P_H(\theta) &= \theta^{c_1}, \text{ for } \theta < \theta_b \\ &= k \cdot \theta^{c_2}, \text{ for } \theta \geq \theta_b, \end{aligned} \quad (10)$$

where θ_b is constant, and $k = \theta_b^{(c_1 - c_2)}$.

To summarize, a statement defining the response of the model at motion threshold has been obtained (equation 8), and the relevant unknowns $r_w \lambda 2(\Delta\theta)$, $P_H(\theta)$, and $p_H(\Delta\theta)$, have been given explicit form.

To fit the observed sinewave motion response

We now fit the theoretical expression of equation 8, to the observed sinewave motion response data of Fig. 5.

Referring to equation 8, it may be seen that with the values of λ available, viz. 180° and 360° , variations in $\Delta\theta_{\min}$ are not significant in determining the relationship of one curve with respect to the other. Thus, for the present, we may assign an arbitrary value to $\Delta\theta_{\min}$ (such that $\Delta\theta_{\min} \leq 13^\circ = \theta_{\min}$ = the minimum value of θ at which f_i may be measured). A specific value is deduced later.

By fitting equation 9 to the $\lambda = 180^\circ$ sinewave response, we obtain $P_H(\theta)$, i.e. the constants c_1 , c_2 , and θ_b of equation 10. The magnitude of the rate constant, a , is obtained by substituting for $P_H(\theta)$, $\Delta\theta_{\min}$, and T_H , and reading off the appropriate value of f_i (it will be remembered that a is only significant at small f_i). Adopting this procedure, equation 8 is fitted to the f_i vs. θ sine data of Fig. 5 for DHF and GF. The results for each observer are displayed in Fig. 11, and the final values of the parameters indicated. The significance of the rate constant, a , at low θ values is evident in the $\lambda = 360^\circ$ response curve, in that values of f_i are reduced in relation to the $\lambda = 180^\circ$ response curve. It is also noted that $P_H(\theta)$, described by the power function of equation 10, provides an adequate fit to the observed data.

Response of the network to square wave stimuli

We now investigate the response of the model to square wave stimuli incident at the inputs.

It was shown earlier that in order for a sensation of well-defined directed motion to be just elicited, it is required that all weighted, H -unit outputs, $r'_{\theta w \lambda}(\Delta\theta)$, have the same sign, and that

$$r'_{\theta w \lambda}(\Delta\theta)_{\max} = T_H \quad (3)$$

where $r'_{\theta w \lambda}(\Delta\theta)$ is defined by equation 2, and $w = 2\pi f_i$.

If the square wave response of Thorson's modification of the Reichardt scheme is evaluated, it is found (FOSTER, 1970) that the H -unit output $r_{w \lambda}(\Delta\theta)$, becomes a function of time (as well as of $\Delta\theta$). (This time dependence arises from the cross-multiplication of the

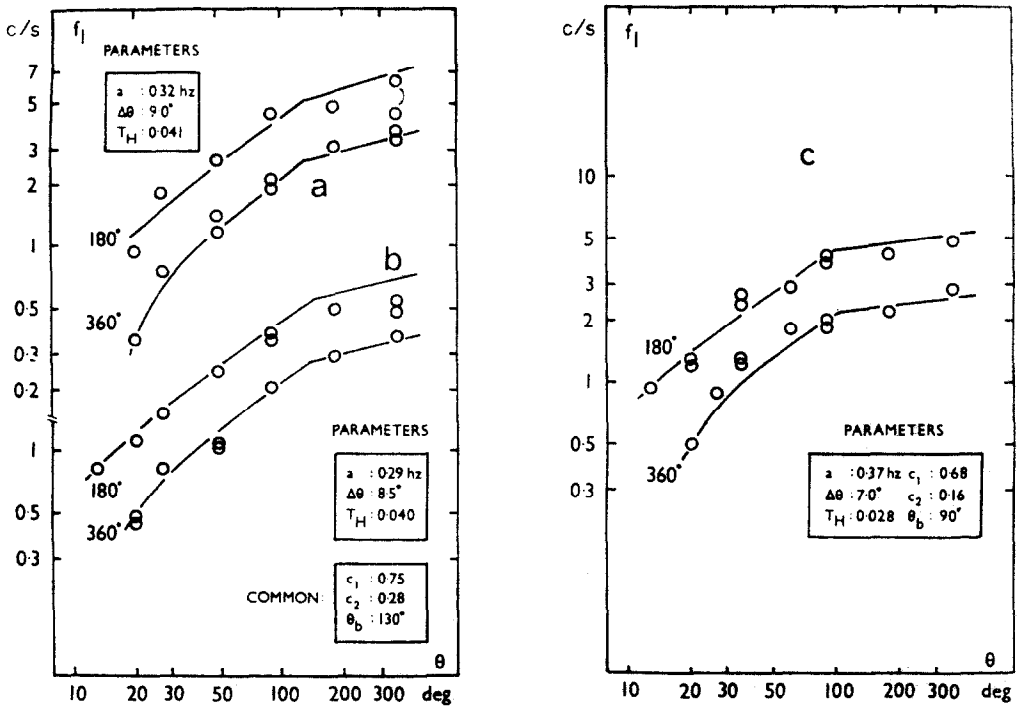


FIG. 11. The theoretical sinewave response of the model (a) and (b) show theoretical fits to the sinewave data of Figs. 5e and 5a, respectively, and (c) shows the theoretical fit to the sinewave data of Fig. 5f. The optimum parameter values are displayed in each case.

sine components of different frequency, present in the square wave stimulus.) Thus, the above threshold condition must be extended to the following requirement, viz. that all $r'_{\theta w\lambda}(\Delta\theta, t)$ have the same sign, and that:

$$r'_{\theta w\lambda}(\Delta\theta, t)_{\max} = T_H \tag{11}$$

where

$$r'_{\theta w\lambda}(\Delta\theta, t) = P_H(\theta) \cdot p_H(\Delta\theta) \cdot r_{w\lambda}(\Delta\theta, t), \tag{12}$$

$r_{w\lambda}(\Delta\theta, t)$ is the square wave response of the H -unit, and the maximum is evaluated with respect to both input pair separation, $\Delta\theta$, and time, t .

If equation 12 is evaluated numerically and the maximum value obtained, it is found (FOSTER, 1970) that at low values of w , $r'_{\theta w\lambda}(\Delta\theta, t)_{\max}$ becomes much greater than T_H , implying values of f_i much greater than those recorded.

Thus, the model in its present form, with Thorson's modification (Fig. 3b) as the H -unit, does not yield a true description of the square wave response, although the sinewave data may certainly be fitted. This failure is directly attributable to the presence of the higher harmonics in the square wave stimulus, and the scheme due to Thorson must be modified to reduce the significance of these harmonics.

The requirements that any modification of the basic scheme must fulfil are therefore the following:

- (1) The sinewave (fundamental) response should remain unaffected.

(2) The response associated with the higher harmonics of the square wave stimulus should be attenuated.

Since the time dependence of the square wave output arises from the presence of the higher harmonics, the simplest (physically realisable) filter with the above properties has the following transfer function:

$$X(s) = \frac{k}{k + s} \tag{13}$$

where s is the complex frequency, and k is a real, positive constant.

The basic network, with this new modification, is shown in Fig. 12.

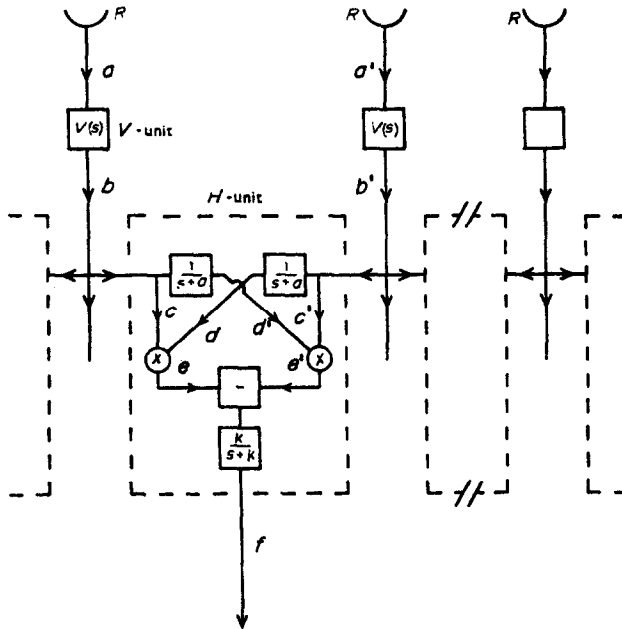


FIG. 12. Representation of the model in the complex frequency domain, showing the detailed structure of the H -unit (q.v. Fig. 2). Note the introduction of output filter, $k/(s + k)$ (see text). The V -units attenuation characteristics, i.e. $|V(s)|$, are given in Fig. 8.

The response of the modified network of Fig. 12 to square wave stimuli

In the Appendix is outlined the derivation of the response of the modified H -unit scheme to square wave inputs. The following expression is obtained:

$$r_{w\lambda}(\Delta\theta, t) = \sum_n \sum_{\substack{n' \\ \text{odd} \\ -\infty}}^{+\infty} \frac{4}{\pi^2} \cdot \frac{e^{j2\pi n\Delta\theta/\lambda}}{nn'} \left[\frac{1}{a + jnw} - \frac{1}{a + jn'w} \right] e^{jw(n+n')t} \cdot \frac{k}{k + j(n + n')w} \cdot W(nw)W(n'w) \tag{14}$$

where $W(w)$ is the V -unit attenuation function, defined by Fig. 8.

Note. The V -units are treated as pure attenuators, weighting each sine component of the input waveform

by the factor, $W(w)$ (see Fig. 12). Any phase shift introduced by the V -units is implicitly included in the properties of the H -unit description.

Now the threshold condition, stated earlier, requires that all weighted outputs, $r'_{\theta w\lambda}(\Delta\theta, t)$, have the same sign, and that:

$$r'_{\theta w\lambda}(\Delta\theta, t)_{\max} = T_H \quad (11)$$

where

$$r'_{\theta w\lambda}(\Delta\theta, t) = P_H(\theta) \cdot p_H(\Delta\theta) \cdot r_{w\lambda}(\Delta\theta, t). \quad (12)$$

Thus, we must first show for this modified scheme that $r'_{\theta w\lambda}(\Delta\theta, t)$, defined by equation 12, with $r_{w\lambda}(\Delta\theta, t)$, defined by equation 14, has the same sign for all accessible values of $\Delta\theta$ and t .

If the RHS of equation 14 is evaluated numerically, and $r_{w\lambda}(\Delta\theta, t)$ obtained as a function of t and $\Delta\theta$, it is found (FOSTER, 1970) that $r_{w\lambda}(\Delta\theta, t)$ is indeed of constant sign for the tested values of $\Delta\theta$ and t .

It is also possible to show (FOSTER, 1970) for a first approximation, that the above is true, analytically, for all $\Delta\theta$ providing that $\lambda \geq 180^\circ$, and for all $\Delta\theta < \lambda/2$, if $\lambda < 180^\circ$. The latter requirements are consistent with the proposed explanation of the stationary stroboscopic effect and the deduced maximum value of $\Delta\theta$, i.e. $60^\circ \leq \Delta\theta_{\max} < 90^\circ$ (see Introduction, and FOSTER, 1969). It is also possible to show that $p_H(\Delta\theta) = \Delta\theta^{-1}$ (i.e. $m = 1$ in equation 4) yields a maximum value of $r'_{\theta w\lambda}(\Delta\theta, t)$ with respect to $\Delta\theta$, at $\Delta\theta = \Delta\theta_{\min}$. This latter result is the same as for the sinewave case.

Thus, the preliminary requirement that all weighted H -unit outputs have the same sign is satisfied. In order to obtain equation 11 in a form which can be related to the observed f_i vs. θ square wave response characteristics, we make the following substitutions into equation 12: $P_H(\theta)$ replaced by the power function of equation 10, $p_H(\Delta\theta)$ by $\Delta\theta^{-m}$ (equation 4), and $r_{w\lambda}(\Delta\theta, t)$ by equation 14. Since $m = 1$ gives a maximum of the weighted output, $r'_{\theta w\lambda}(\Delta\theta, t)$, with respect to $\Delta\theta$ at $\Delta\theta_{\min}$ (see earlier), it merely remains to obtain the maximum with respect to t of $r'_{\theta w\lambda}(\Delta\theta_{\min}, t)$, or equivalently $r_{w\lambda}(\Delta\theta_{\min}, t)$, from equation 14.

Therefore, rearranging equation 11, we arrive at the following expression:

$$\begin{aligned} \theta &= \exp \left[\frac{1}{c_1} \cdot \ln \left\{ T_H / \frac{1}{\Delta\theta_{\min}} \cdot r_{w\lambda}(\Delta\theta_{\min}, t)_{\max} \right\} \right], & \text{for } \theta < \theta_b \\ &= \exp \left[\frac{1}{c_2} \cdot \ln \left\{ \left(T_H / \frac{1}{\Delta\theta_{\min}} \cdot \theta_b^{c_1 - c_2} \cdot r_{w\lambda}(\Delta\theta_{\min}, t)_{\max} \right) \right\} \right], & \text{for } \theta \geq \theta_b \end{aligned} \quad (15)$$

providing that if $\lambda < 180^\circ$, $\theta < \lambda/2$.

Now, values of the constants T_H , θ_b , c_1 , c_2 , and a in equation 14, have already been derived in the sinewave analysis; trial values of $\Delta\theta_{\min}$ ($\Delta\theta_{\min} = 13^\circ$) and the rate constant k ($k \sim a$) may be assigned, and the right hand side of equation 15 then evaluated numerically.

In this manner, the square wave f_i vs. θ data of Fig. 5 for DHF and GF are fitted. The constants k and $\Delta\theta_{\min}$ can be uniquely determined, since each has a distinct effect upon the response characteristics: k on the low frequency (long λ) end of the response and $\Delta\theta_{\min}$ on the short λ end. In Fig. 13a theoretical fits to the f_i vs. θ sine and square wave data of Fig. 5a (for DHF) with $\lambda = 180^\circ$ and 360° , are shown together. Identical parameter values are used for this set, since the sine and square wave results were recorded in the same session. In

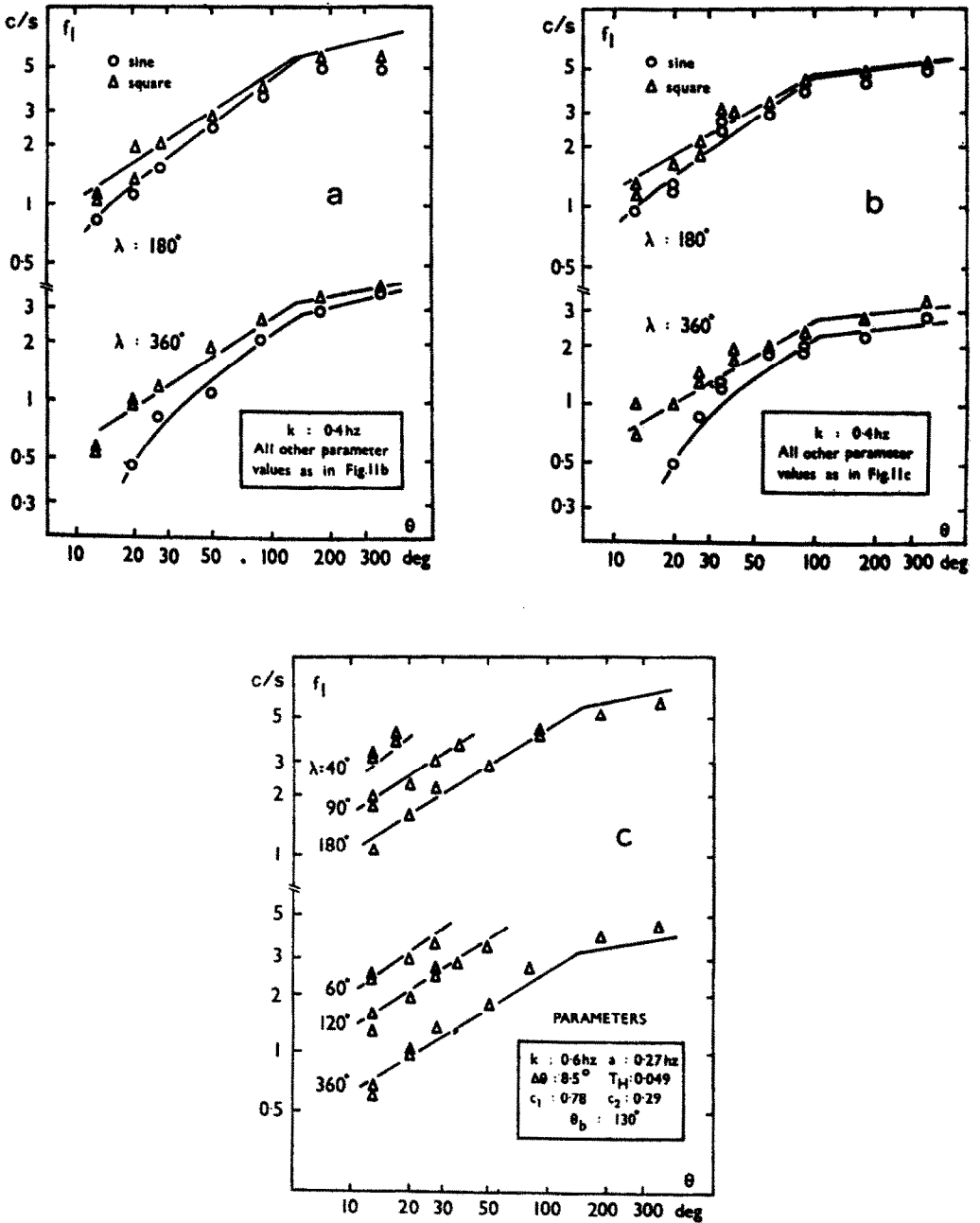


FIG. 13. The theoretical square wave response of the model. In (a) is shown the theoretical fit to the sine and square wave data of Fig. 5a; in (b) is shown the theoretical fit to the square wave data of Fig. 5d and to the sinewave data of Fig. 5f; in (c) is shown the theoretical fit to the square wave data of Fig. 5c. The relevant parameter values are indicated in each case (see text).

Fig. 13b, a similar comparison between fits to the sine and square wave data of Figs. 5d and 5f (for GF) is shown; identical parameter values were again used, although in this case sine and square wave data were obtained in different sessions.

Finally in Fig. 13c is shown the theoretical fit to the square wave data of Fig. 5c (for DHF) with λ taking on all experimental values from 360° to 40° .

In all cases, the relevant parameter values are indicated.

The minimum input pair separation, $\Delta\theta_{\min}$

In the previous section, values of the rate constant, k , and the minimum input pair separation, $\Delta\theta_{\min}$, were obtained; the latter was determined, however, for only one set of data values (Fig. 13c). In this section, a specific determination of $\Delta\theta_{\min}$ is made using experimental data values for $\theta = \theta_{\min} = 13^\circ$, only. In this way, it is possible to evaluate more directly, the effect of variation in $\Delta\theta_{\min}$ on the response shape.

The following method is used to determine the optimum value of $\Delta\theta_{\min}$.

Equation 15, describing the square wave motion response, is solved for all experimental values of λ (40° – 360°), with various values of $\Delta\theta_{\min}$. All other parameter values are fixed from previous analyses. The resulting theoretical values of the f_i vs. λ response, for fixed θ ($\theta = 13^\circ$), are then compared with the observed square wave, f_i vs. λ response data, obtained by "sampling" the f_i vs. θ curves (Fig. 5) at $\theta = 13^\circ$.

Note. The choice of value for $\Delta\theta_{\min}$ is only significant at small λ . This may be seen from the following. (a) With sine stimuli, the H -unit response, given by equation 5, contains the term, $\sin(2\pi \cdot \Delta\theta/\lambda)$. If

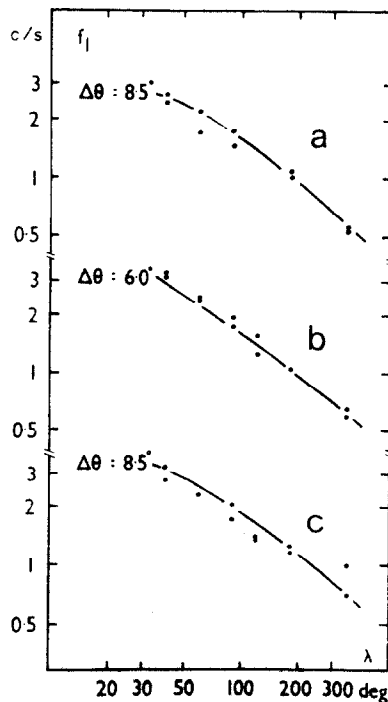


FIG. 14. Optimum values of the minimum input (receptor) pair separation, $\Delta\theta_{\min}$. In (a) is shown the fit of the theoretical f_i vs. λ squarewave response, at $\theta = 13^\circ$, to the data of Fig. 5a. In (b) and (c) are shown the fits to the data of Figs. 5c and 5d (see text).

$\Delta\theta = \Delta\theta_{\min} \ll \lambda$, $\sin(2\pi\Delta\theta_{\min}/\lambda)$ may be replaced by its argument, $(2\pi\Delta\theta_{\min}/\lambda)$, and therefore providing $\lambda \gg \Delta\theta_{\min}$, variations in $\Delta\theta_{\min}$ affect all outputs similarly, *independently* of λ .

(b) For square wave stimuli, similar arguments apply. Thus, referring to equation 14, it may be seen that choice of $\Delta\theta_{\min}$ is only significant when we can no longer write $n\Delta\theta_{\min} \ll \lambda$. For the case of λ large, this only fails if n is also large, where the associated attenuation is also high (see Fig. 8). It then follows that as in (a), the choice of $\Delta\theta_{\min}$, for large λ , is not significant in determining the shape of the f_i vs. λ response.

Any bodily shift in f_i vs. λ curves, associated with changes in $\Delta\theta_{\min}$, may therefore be corrected by adjusting T_H for optimum fit at the long λ end.

In this manner, optimum values of $\Delta\theta_{\min}$ are obtained with reference to the data drawn from Figs. 5a, c, d (for DHF and GF). The best fits and associated $\Delta\theta_{\min}$ values are shown in Fig. 14. For DHF, $\Delta\theta_{\min} = 6.0^\circ$ and 8.5° , and for GF, $\Delta\theta_{\min} = 8.5^\circ$.

Predictions of the model

We now discuss some predictions of the model, with particular reference to the phase-sensitivity of the system.

It was stated in the Introduction, that the basic Reichardt scheme (Fig. 3a) exhibits the property of phase insensitivity, i.e. the response of the system is independent of the phase relationships of the Fourier components making up the stimulus pattern. (It should be noted that the phase insensitivity described here is distinct from the spatial phase insensitivity of the V-unit summation/threshold system referred to in the Introduction.) This phase insensitivity of the Reichardt multiplier is directly attributable to presence of the time-averaging element (see Fig. 3a), which renders the output time-invariant.

In the present scheme, Fig. 12, with filter, $k/(s+k)$, on each output, there exist two components to the general motion response, viz: a time invariant component, which is insensitive to the phase structure of the stimulus pattern, and a time-dependent component, which is *not* insensitive to the phase structure of the stimulus pattern (FOSTER, 1970). As the temporal frequency (i.e. $|s|$) increases, the time-varying component is progressively attenuated, and with it, the phase sensitivity of the system.

We therefore have the following:

At low temporal frequencies, (i.e. low f_i) the model exhibits phase sensitivity to the stimulus structure. At high temporal frequencies (i.e. high f_i) it does not.

These predictions of the model were examined using a symmetry test (see FOSTER, 1970), and were shown to be true for two naive observers. [These findings are not inconsistent with the earlier deduction that the system is phase insensitive (FOSTER, 1969), since this was established for large θ i.e. high temporal frequencies.]

DISCUSSION

We now examine some of the general properties of the system model and their implications with respect to the human visual system.

The input (receptor) pair separation of the model

It has been shown that the model, describing the visual system in its motion response, has input (receptor) pair separations, $\Delta\theta$, ranging from a minimum, $\Delta\theta_{\min}$, of approximately 8° , to a maximum, $\Delta\theta_{\max}$, of between 60° and 90° (the angular separation, $\Delta\theta$, being measured around the annular field).

Thus, to restate the results obtained earlier (FOSTER, 1969), the human visual system *behaves* as if interaction leading to motion perception can take place between receptors (or groups of receptors) separated by up to ten times the minimum interaction distance. This

contrasts with the results of Hassenstein, Reichardt and Varju (REICHARDT and VARJU, 1959) for the beetle *Chlorophanus*. In the latter, interaction leading to motion perception is found not to extend much beyond adjacent ommatidia.

The time constants of the filters

For the final version of the model (Fig. 12), the values of the rate constants, a , for the cross filters, and k , for the output filter, were determined to be approximately $0.3 (\times 2\pi \text{ rad./s})$ and $0.5 (\times 2\pi \text{ rad./s})$ respectively, for both DHF and GF (see Fig. 13). If the corresponding time constants are $T_a (T_a = 1/a)$ and $T_k (T_k = 1/k)$ then $T_a \sim 0.5$ (sec) and $T_k \sim 0.3$ (sec).

Now the constants a and k , occur in filters with transfer functions of the form $1/(s + a)$, where s is the complex frequency. In the full derivation of the motion response of the model (FOSTER, 1970) it is shown that these filters give rise to transient terms, the amplitudes of which fall off as e^{-at} or e^{-kt} . To extract the steady state component from the general solution for the motion response, t must be made sufficiently large in order that these transient terms can be neglected, i.e. $t \gg T_a, T_k$.

This theoretical requirement for steady state conditions is consistent with the experimental observation that steady state motion sensation is usually achieved within about five seconds (FOSTER, 1969). The latter period is approximately ten times the greatest time constant defined above.

Further implications of the model

One consequence of the model is the following:

Two fixed, time-varying input signals, with appropriate phase difference and angular separation, $\Delta\theta$, will produce a non-zero motion response from the relevant H -unit(s). Thus, qualitatively, the model predicts the existence of the phi-phenomenon (WERTHEIMER, 1912); that is, under certain conditions, two stationary flashing light sources, with suitable time-lag and spatial separation, will give rise to a sensation of motion between the two sources.

It is noted that this sensation of motion will be produced in exactly the same way as a continuous moving stimulus induces a sensation of motion. This is consistent with the arguments of WERTHEIMER (1912), BROWN (1931) and GIBSON (1954) and with the experimental findings of GRÜSSER, GRÜSSER-CORNEHLS and LICKER (1968) in the frog.

A second implication of the model is in relation to the existence of a lower speed limit for motion perception.

Referring to equation 8, describing the sinewave response of the model, it may be seen that for any value of the angular area, θ (such that $\theta > \theta_{\min}$, the minimum area for which f_i may be recorded), there exist two solutions for the temporal frequency, w , i.e. the two roots of the equation:

$$\frac{w}{w^2 + a^2} = \text{constant} \quad (16)$$

where $w = 2\pi f$.

If these two roots are w_1 and w_2 , with $w_1 < w_2$, then for any w such that $w_1 \leq w \leq w_2$, a sensation of well defined directed motion is induced, since for this range of frequencies, the LHS of equation 16 is greater than or equal to the threshold constant, T_H .

Now w_2 is the previously defined lower critical frequency, i.e. $w_2 = 2\pi f_l$, and this provides an upper limit on the range of directed motion sensation; w_1 , in contrast, provides a lower limit on the range of directed motion sensation.

Thus, the model predicts that if the temporal frequency of the moving stimulus is steadily reduced, there exists a frequency (w_1) below which a sensation of well-defined directed motion cannot be induced.

This is consistent with the observations of AUBERT (1886) and BROWN (1931).

CONCLUSION

An investigation has been carried out into the response of the human visual system to certain classes of moving spatially-periodic stimuli. The principal characteristics of the response have been shown common to several subjects, and a mathematical model, describing the system in this response, has been constructed. The model was tested and its validity confirmed.

It is emphasised that the conclusions reached in this investigation are strictly valid only for the class and configuration of inputs defined—although it has been indicated that the model may have implications with respect to other well established phenomena, viz, the phi-phenomenon and the lower speed limit for motion perception.

REFERENCES

- AUBERT, H. (1886). Die Bewegungsempfindung. *Arch. ges. Physiol.* 39, 347-370.
- BROWN, J. F. (1931). The thresholds for visual movement. *Psychol. Forsch.* 14, 249-268.
- DITCHBURN, R. W. and GINSBURG, B. L. (1953). Involuntary eye-movements during fixation. *J. Physiol.* 119, 1-17.
- DEN, H. DE LANGH (1954). Relation between critical flicker frequency and a set of low frequency characteristics of the eye. *J. opt. Soc. Am.* 44, 380-389.
- FOSTER, D. H. (1968). The perception of moving spatially-periodic, intensity distributions. *Optica Acta* 15, 625-626.
- FOSTER, D. H. (1969). The response of the human visual system to moving spatially-periodic patterns. *Vision Res.* 9, 577-590.
- FOSTER, D. H. (1970). Some experiments on the detection of motion by the human visual system and their theoretical interpretation. Ph.D. Thesis, University of London.
- GIBSON, J. J. (1954). The visual perception of objective motion and subjective movement. *Psychol. Rev.* 61, 304-314.
- GILBERT, D. S. and FENDER, D. H. (1969). Contrast thresholds measured with stabilized and non-stabilized sine-wave gratings. *Optica Acta* 16, 191-204.
- GRÜSSER, O. J., GRÜSSER-CORNEHLS, U. and LICKER, M. D. (1968). Further studies on the velocity function of movement detecting class-2 neurons in the frog retina. *Vision Res.* 8, 1173-1186.
- LORD, M. P. and WRIGHT, W. D. (1950). The investigation of eye movements. *Rep. Prog. Phys.* 13, 1-23.
- MC LACHLAN, N. W. (1963). *Complex Variable Theory and Transform Calculus*, Cambridge University Press, Cambridge.
- REICHARDT, W. and VARJU, D. (1959). Übertragungseigenschaften im Auswertesystem für das Bewegungsehen. *Z. Naturforsch.* 14b, 674-689.
- RIGGS, L. A., RATLIFF, E., CORNSWEET, J. C. and CORNSWEET, T. N. (1953). The disappearance of steadily fixated test objects. *J. opt. Soc. Am.* 43, 495-501.
- THORSON, J. (1966). Small angle analysis of a visual reflex in the locust. *Kybernetik* 3, 41-66.
- WERTHEIMER, M. (1912). Experimentelle Studien über das Sehen von Bewegung. *Z. Psychol.* 61, 161-265.
- WEST, D. C. (1968). Effect of retinal image motion on critical flicker-fusion measurement. *Optica Acta* 15, 317-328.

APPENDIX

Referring to Fig. 12, let square wave, $f(t)$, of unit amplitude and period T , be incident at (a), and let $f(t + \Delta t)$ be incident at (a'). Transforming to the Laplace domain,

$$\text{if } f(t) \rightarrow F(s)$$

$$\text{and } f(t + \Delta t) \rightarrow F(s)e^{s\Delta t}$$

s is the complex frequency, and $F(s) = \frac{1}{s} \left[\frac{1 - e^{-sT/2}}{1 + e^{-sT/2}} \right]$

Transmission of the signal through the V units, each with transfer function $V(s)$, gives at (b): $V(s) \cdot F(s)$ and at (b'): $V(s) \cdot F(s)e^{s\Delta t}$.

At (c), the signal remains the same as that at (b), but because of the cross-filter, $1/(s+a)$, we obtain at (d):

$$\frac{1}{s+a} \cdot V(s) \cdot F(s) e^{s\Delta t}.$$

At (e) and (e'), the two signals are multiplied together in the time domain. In the complex frequency domain, this is equivalent to convolution, which is represented here by the operation, *.

Thus at (e) we have:

$$[V(s) \cdot F(s)] * \left[\frac{1}{s+a} \cdot V(s) \cdot F(s) e^{s\Delta t} \right]$$

and, similarly, at (e'), we have:

$$\left[\frac{1}{s+a} \cdot V(s) \cdot F(s) e^{s\Delta t} \right] * [V(s) F(s) e^{s\Delta t}].$$

Let the difference of the above two expressions be $R'(s)$. Then substituting for $F(s)$, and writing the convolution in full, we get the following contour integral for $R'(s)$:

$$R'(s) = \frac{1}{2\pi j} \int_{\sigma-j\infty}^{\sigma+j\infty} V(s') \cdot \frac{1}{s'} \cdot \frac{1 - e^{-s'T/2}}{1 + e^{-s'T/2}} \cdot V(s-s') \cdot \frac{1}{s-s'} \cdot \frac{1 - e^{-(s-s')T/2}}{1 + e^{-(s-s')T/2}} \cdot e^{s'\Delta t} \cdot \left[\frac{1}{s'+a} - \frac{1}{(s-s')+a} \right] d's'$$

where $O < \sigma < \text{real part of } s$.

Converting the above expression to a closed contour, and appealing to the residue theorem (see, for example, MCLAULAN, 1963), yields the following for $R'(s)$:

$$R'(s) = \sum_{\substack{n \\ \text{odd} \\ -\infty}}^{\infty} V(jnw) \cdot \frac{1}{jnw} \cdot \frac{4}{T} \cdot V(s-jnw) \cdot \frac{1}{s-jnw} \cdot \frac{1 + e^{-sT/2}}{1 - e^{-sT/2}} \cdot e^{jnw\Delta t} \left[\frac{1}{jnw+a} - \frac{1}{s-jnw+a} \right].$$

The final output, $R(s)$ say, is obtained after transmission of the above through the output filter, $k/(s+k)$, thus:

$$R(s) = R'(s) \cdot \frac{k}{s+k}.$$

Transforming the above expression back into the time domain, we arrive at the following expression for the steady state output, $r_{w\lambda}(\Delta\theta, t)$.

$$r_{w\lambda}(\Delta\theta, t) = \sum_n \sum_{\substack{\pi \\ \text{odd} \\ -\infty}}^{\infty} \frac{4}{\pi^2} \cdot \frac{e^{j2\pi n\Delta\theta/\lambda}}{nn'} \left[\frac{1}{a+jnw} - \frac{1}{a+jn'w} \right] \cdot e^{jw(n+n')t} \cdot \frac{1}{k+j(n+n')w} \cdot W(nw) W(n'w)$$

where $V(jnw)$ has been replaced by its modulus, $W(nw)$, defined by Fig. 8, and $w\Delta t$ has been replaced by $2\pi\Delta\theta/\lambda$.

Note. In performing the operations of convolution and inverse transformation, the steady state components of the solution, only, were considered. The transient terms, falling off as $e^{-\sigma t}$ or $e^{-\lambda t}$, were ignored.

Abstract—This study is a continuation of an earlier investigation (FOSTER, 1969) into the response of the human visual system to moving spatially-periodic stimuli. Experimental data are presented for several observers, and a detailed analysis is then carried out. A specific mathematical structure is given to the system model and theoretical fits to both sine and square wave motion response data are obtained. It is shown that the model has implications with respect to the interaction distance of receptor units, and to the existence of the phi-phenomenon and the lower speed limit for motion perception.

Résumé—Ce travail continue une recherche antérieure (FOSTER, 1969) sur la réponse du système visuel humain à des stimuli mobiles à périodicité spatiale.

On présente les résultats expérimentaux de plusieurs observateurs, et on les analyse en détail. On donne une structure mathématique spécifique au système de modèle, ce qui permet un accord théorique à la fois avec les données de réponse au mouvement pour des ondes sinusoidales et carrées.

On montre que ce modèle a des implications en rapport avec la distance d'interaction des unités réceptrices, avec l'existence du phénomène phi et avec la limite inférieure de vitesse pour la perception de mouvement.

Zusammenfassung—Diese Versuche sind eine Fortsetzung einer früheren Untersuchung (FOSTER, 1969) der Antwort des menschlichen Gesichtssinnes auf raumperiodische Bewegungareize. Es werden Versuchsergebnisse für einige Beobachter geliefert und hierauf wird eine einschlägige Analyse ausgeführt. Es wird ein mathematisches Gerüst für das Systemmodell erbaut und es werden Anpassungen für die Sinus- und Rechteckwellenbewegungsantworten gewonnen. Es wird gezeigt, dass das Modell über die Wechselspielentfernung der Rezeptoreinheiten und die Existenz des θ -Phänomens und der niederen Geschwindigkeitschranke für die Bewegungswahrnehmung auszusagen vermag.

Резюме — Эта работа является продолжением прежнего исследования (FOSTER, 1969) реакций зрительной системы человека на движения пространственно-периодических стимулов.

Представлены экспериментальные данные для нескольких наблюдателей и затем произведен детальный анализ их.

Даются специальные математические построения для модели этой системы и получено теоретическое соответствие реакций на движение как для синусоидальных, так и для квадратных волн.

Показано, что модель имеет в виду дистантное взаимодействие рецепторных единиц и имеет отношение к существованию фи-феномена и более низкой пороговой скорости при восприятии движения.